

ACCELERATING FATIGUE INDUCED CRACK PROPAGATION MODELING IN CONCRETE USING THE TIME HOMOGENIZATION APPROACH

R. PINA-TORRES *, D. ZHAO * AND M. KALISKE*†

* Institute for Structural Analysis, Technische Universität Dresden
01062 Dresden, Germany

† corresponding author: michael.kaliske@tu-dresden.de

Key words: High-cycle fatigue, phase-field method, time homogenization, computational efficiency, crack propagation

Abstract. In this contribution, a time homogenization (TH) scheme is utilized to accelerate the computational simulation of fatigue induced crack propagation in engineering materials, specifically focusing on concrete subjected to cyclic loads. The proposed approach segregates the problem into distinct micro- and macro-time scales, improving computational efficiency by extrapolating internal variables linked to material fatigue. This method, originally applied to multi-scale problems such as tire life cycle analysis, is now adapted to model fatigue induced damage in concrete structures.

The model is built on a modified phase-field formulation that considers material degradation due to fatigue and the Representative Crack Element formulation as an energy split. The time homogenization accelerates the simulation by upscaling micro-scale behavior over extended macro-time periods. The model performance has been previously tested against high-fidelity simulations and it has been demonstrated the method's potential to effectively model crack growth under various loading conditions. The novelty of this approach lies in its application of a methodology based on computational homogenization to fracture mechanics. By utilizing this framework, the computational burden is significantly reduced, providing results that approximate high-fidelity simulations with much shorter processing times. In this contribution, the time homogenization scheme is extended to experimental validation, utilizing data from fatigue tests. A comparison between simulation results and experimental observations is presented, demonstrating the method's accuracy in replicating crack growth patterns and fatigue behavior. The results confirm that the time homogenization approach offers a reliable and efficient alternative to traditional methods, particularly in high-cycle fatigue cases, reducing computational time without sacrificing accuracy.

1 Introduction

Fatigue fracture, characterized by progressive damage accumulation leading to failure under cyclic loading, poses significant challenges in engineering. Accurate modeling of fatigue induced damage and crack propagation are critical for ensuring structural integrity and reliability.

Traditional methodologies for addressing fa-

tigue failure extend the foundational phase-field formulation, proposed by [1], with additional terms to capture fatigue degradation effects, as developed in [2], [3], and [4]. However, these approaches face challenges due to the high computational cost associated with resolving fine scale crack propagation and managing the additional degrees of freedom required across numerous loading cycles.

The computational burden of performing phase-field simulations for each loading cycle limits their feasibility in practical engineering applications. To overcome these limitations, various strategies have been proposed, including cycle jump techniques by [5] and [6], as well as TH or multi-scale approaches as in [7] and [8] for fatigue modeling.

This study introduces a TH designed for phase-field formulations in fatigue fracture analysis. Building on methods initially proposed by [9] for long-term response analysis of asphalt pavements and by [10] for dynamic loading of footings, this TH approach significantly reduces computational demands while maintaining predictive accuracy. By accelerating the simulation of fatigue induced damage, the method enables efficient exploration of various loading scenarios and design parameters.

2 Theoretical background

2.1 Phase-field formulation for brittle fracture

The phase-field approach for elastic brittle fracture models the system's total energy functional as

$$E_{\text{total}} = \int_{\Omega \setminus \Gamma} \psi \, d\Omega + G_c \int_{\Gamma} dA - E_{\text{ext}}. \quad (1)$$

As shown in Figure 1, Ω is the material domain, and Γ denotes the crack surface. The material's fracture toughness is given by G_c . The energy functional also includes the external contributions E_{Ext} , as the contributions from external forces and body forces.

The fracture energy can be regularised into a volume integral, incorporating a crack density function γ_l . The Representative Crack Element (RCE), as presented in Section 2.2, is used as a physics based approach for the energy split method, leading to

$$E_{\text{total}} = \int_{\Omega} [\psi^{\text{crack}} + g(d) (\psi^{\text{solid}} - \psi^{\text{crack}})] \, d\Omega + G_c \int_{\Omega} \gamma_l(d) \, d\Omega - E_{\text{ext}} \rightarrow \min, \quad (2)$$

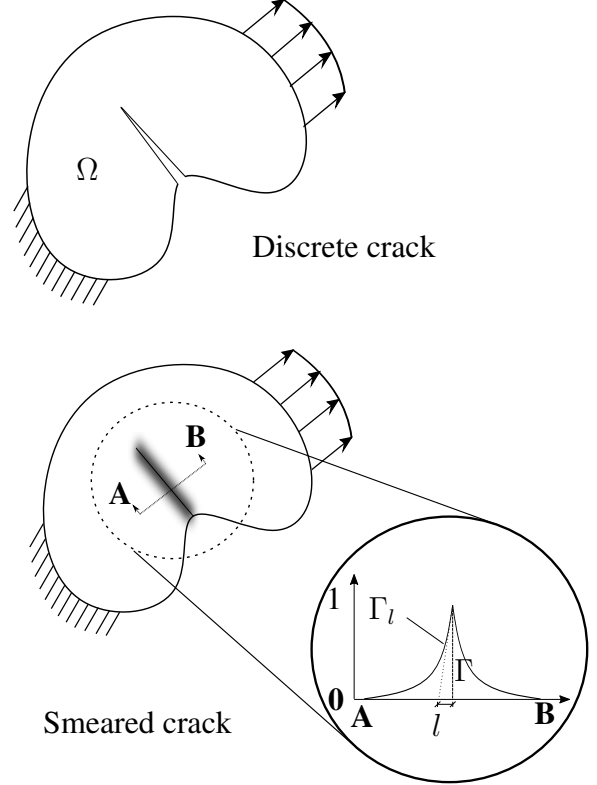


Figure 1: Profile of the phase-field through a crack.

where $g(d)$ is the degradation function and d is the phase-field variable representing damage (ranging from 0 for intact to 1 for fully damaged material).

To account for fatigue effects, an additional degradation function $f(\bar{\alpha})$ is defined and it modifies the fracture energy, reducing $G_{c,0}$ to $G_c = f(\bar{\alpha}) \cdot G_{c,0}$ according to the material's loading history. The damage driving energy α is

$$\alpha = g'(d) (\psi^{\text{solid}} - \psi^{\text{crack}}), \quad (3)$$

and the cumulative fatigue damage $\bar{\alpha}(x, t)$ is integrated over time, considering only the loading phases, where $\dot{\alpha} \geq 0$. The fatigue degradation function $f(\bar{\alpha})$ is adapted based on the accumulated damage, as described in [2].

2.2 Representative Crack Element (RCE)

This study adopts the RCE framework introduced in [11] and [12]. This approach is preferred as it provides a specialized method for describing material behavior in the presence of cracks, complementing conventional mate-

rial models used for intact materials, denoted as ψ^{solid} . The RCE framework enables the characterization of crack behavior through a physically grounded model. RCEs are continuum mechanical models designed to represent cracks discretely via computational homogenization, integrated with the phase-field model. In this approach, each RCE encompasses a small representative section of a discrete crack, where the crack is assumed to be approximately planar, and the bulk displacement gradient is nearly homogeneous. As depicted in Figure 2, the RCE domain, $\bar{\mathcal{B}}$, is symmetrically divided into two subdomains, $\bar{\mathcal{B}}^1$ and $\bar{\mathcal{B}}^2$, separated by the crack surface $\bar{\mathcal{B}}^\Gamma$.

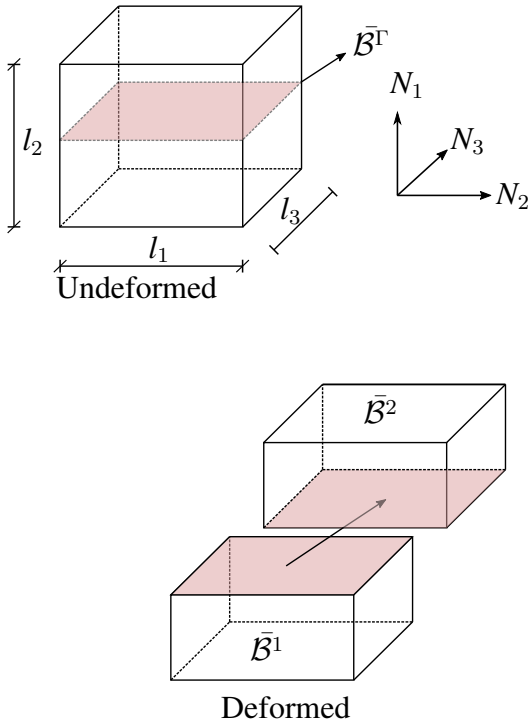


Figure 2: Representation of an RCE in undeformed and deformed states.

The detailed mathematical formulation of the RCE method is beyond the scope of this study and can be found in [11].

2.3 Time Homogenization (TH)

TH is an algorithm designed to address systems with distinct temporal multiscale characteristics by separating them into micro and macro time scales, as depicted in Figure 3.

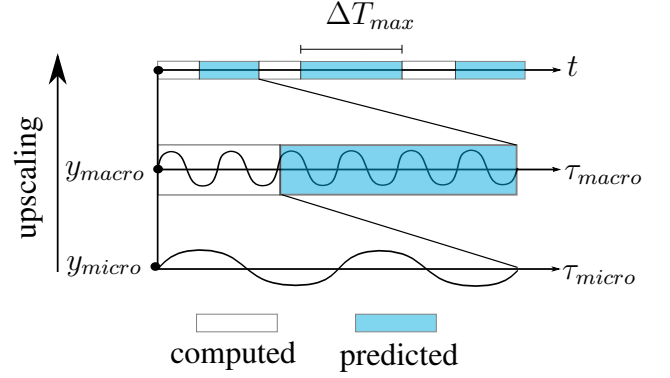


Figure 3: Representation of the different time scales.

As outlined in [13], the process begins with high-resolution simulations to analyze the evolution of internal variables, \mathbf{y} , over a representative micro time period, τ_{micro} . From these simulations, the homogenized rate of change of internal variables, $\langle \dot{\mathbf{y}}_0 \rangle$, is computed, encapsulating the system's key characteristics. This is expressed as

$$\langle \dot{\mathbf{y}}_0 \rangle = \frac{1}{\tau_{micro}} \int_0^{\tau_{micro}} \dot{\mathbf{y}}(\tau) d\tau. \quad (4)$$

The macro time computation is then carried out through a sequence of micro and macro steps. During the micro step, internal variables are extrapolated, while the macro step ensures equilibrium. The size of each macro time step, ΔT_{max} , is adaptively determined based on the sensitivity of the internal variables. The primary goal is to accurately capture the dominant behavior and characteristics of the system's internal variables, achieving computational efficiency without compromising the system's essential features.

3 Numerical examples

3.1 Ballastless track systems

Ballastless track systems are an alternative form of railway infrastructure designed to provide greater stability, durability, and reduced maintenance compared to traditional ballasted tracks. Instead of using loose ballast to support and distribute loads, ballastless tracks consist of a rigid concrete or mortar layer that directly anchors the rails. This configuration offers sev-

eral advantages, including improved resistance to dynamic and static loads, enhanced alignment retention, and suitability for high-speed trains. An illustration of the structure of a ballastless track system is shown in Figure 4.

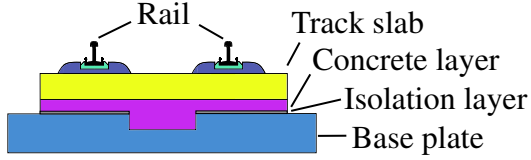


Figure 4: Structure of a ballastless track system.

The numerical study in this work is based in the experimental data presented in [14], [15] and [16], where the concrete used in concrete layer (see Figure 4) is analyzed. To assess the material's mechanical behavior, the study incorporates two types of loading conditions: monotonic and cyclic fatigue. These experimental results serve as a benchmark for validating the numerical simulations, allowing comparisons between the observed experimental outcomes and simulated results for both monotonic and cyclic loading cases.

Figure 5 illustrates the dimensions, geometry and boundary conditions of the test specimens used in the experiments and in the simulations. It consists of a beam subjected to four points bending test.

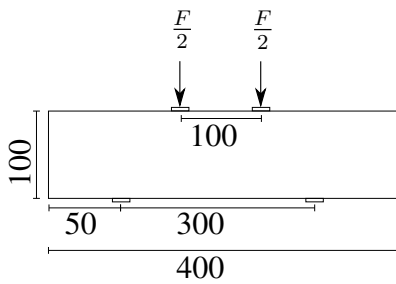


Figure 5: Dimensions of the concrete specimens (all units in mm).

3.1.1 Monotonic test

The monotonic test involved applying a steadily increasing load to the specimen until failure. This test provided a basis for parameter calibration in the simulations, allowing for the

determination of key material properties. Poisson's ratio is set to $\nu = 0.3$, the elastic modulus is $E = 32.5$ GPa, and the energy release rate is calibrated to $G_c = 0.03$ N/mm².

The ultimate flexural strength f_f is calculated as

$$f_f = \frac{Fl}{bh^2}, \quad (5)$$

where F is the ultimate load, l is the span between supports, and b and h are the width and height of the specimen.

The average ultimate flexural strength obtained from the experiments is 5.77 MPa, with a variability band of $\pm 15\%$, as defined by the authors. In the simulation, the maximum flexural strength achieved is 5.65 MPa, which falls within this range, confirming the model's accuracy in simulating the material's behavior under static loading.

3.1.2 Cyclic fatigue test

The cyclic fatigue test involved subjecting the specimens to repeated loading and unloading cycles to simulate the dynamic conditions experienced in ballastless track systems. The loading pattern for the cyclic fatigue test is shown in Figure 6.

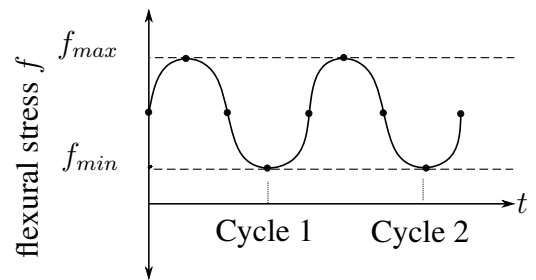


Figure 6: Load pattern.

The stress levels S_{max} and S_{min} , as depicted, are calculated using the equations

$$S_{max} = \frac{f_{max}}{f_a} \quad (6)$$

and

$$S_{min} = \frac{f_{min}}{f_a}. \quad (7)$$

Here, f_a represents the average flexural strength of the specimen and f_{min} and f_{max} the associated flexural strength for a target stress level. For analysis purposes, the experimental procedure defined five different groups based on the S_{max} values: 0.65, 0.7, 0.75, 0.8, and 0.85, each with a constant corresponding S_{min} of 0.1, according to the experimental plan proposed by [15].

Following the cyclic fatigue tests, the numerical results are compared to the experimental results using an S-N curve, which plots the maximum stress levels, S_{max} , against the number of cycles to failure, $\log(N)$. The S-N curve is important because it provides a graphical representation of the relationship between stress and fatigue life, allowing to predict the number of cycles a material can withstand under a given stress level before failure occurs. This curve is fundamental for understanding material behavior under cyclic loading, as it helps to identify the fatigue limit, to assess the durability of materials, and to optimize designs to prevent premature failure. This comparison is illustrated in Figure 7.

3.2 Efficiency of Time Homogenization

The performance of the time homogenization scheme proved to be effective, as it demonstrates good agreement with the experimental results. This method allows for a more streamlined approach, avoiding the need to simulate every individual cycle. The efficiency gains are significant, as shown in Table 1, which details the computational cost savings for each stress group.

	Number of simulations		
	$S_{max} = 0.75$	$S_{max} = 0.80$	$S_{max} = 0.85$
Full Case [-]	24943	9528	4965
TH [-]	3018	1622	1048
Savings [%]	87.9	83.0	79.9

Table 1: Computational cost savings achieved using the time homogenization scheme for different stress groups.

By applying time homogenization, the simulations are completed with reduced computational resources, maintaining the accuracy of results comparable to the experiments.

4 Conclusions and outlook

The implementation of the time homogenization scheme in the simulation of fatigue-induced crack propagation shows promising results, though further refinement is needed. Preliminary results demonstrate a strong agreement with experimental data, suggesting the potential for a reliable and accurate approach. Notably, the method offers substantial computational cost savings, as illustrated in Table 1. By reducing the need to simulate each individual step, the time homogenization approach has shown to significantly decrease computational effort while maintaining sufficient precision for life prediction. This efficiency paves the way for large-scale simulations with more limited resources.

However, additional work is required, particularly in refining the degradation function to better capture the behavior of the mortar under fatigue loading. Once this aspect is fully addressed, the approach is expected to provide an even more robust and comprehensive tool for structural analysis.

5 Acknowledgements

This work is funded by the Deutsche Forschungsgemeinschaft (DFG) through the the Priority Program 2020 ‘‘Cyclic Deterioration of High-Performance Concrete in an Experimental-Virtual Lab’’, project-ID 352324592, ka 1163/40. The financial support is gratefully acknowledged.

References

- [1] B. Bourdin, G. Francfort, and J.-J. Marigo, 2000, Numerical experiments in revisited brittle fracture, *Journal of the Mechanics and Physics of Solids* **48**: 797–826.
- [2] P. Carrara, M. Ambati, R. Alessi, and L. De Lorenzis, 2020, A framework to

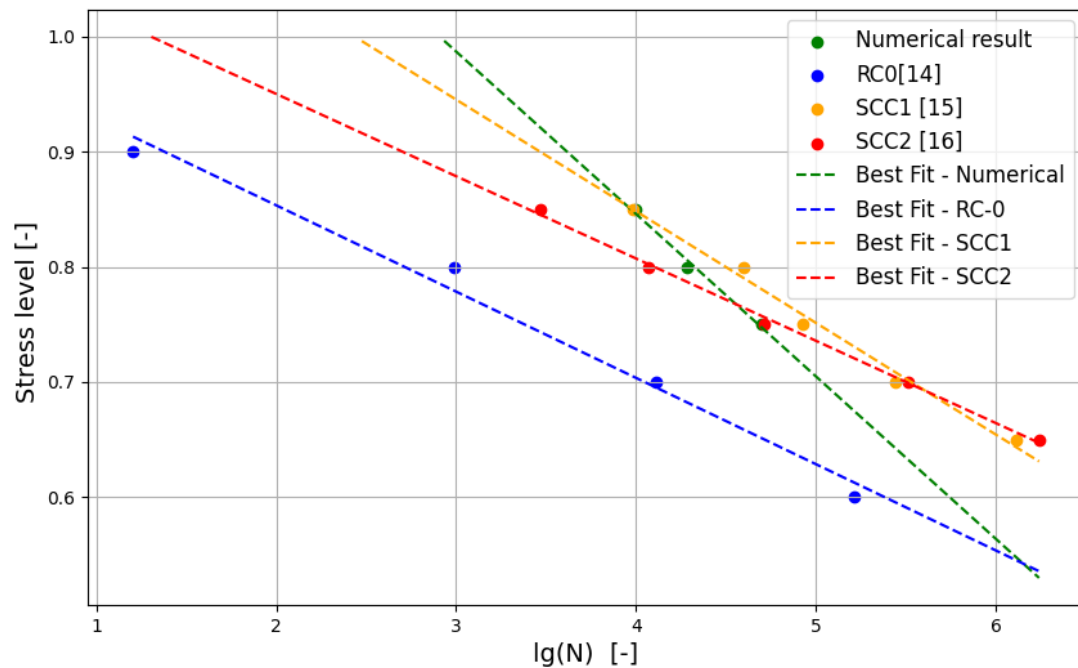


Figure 7: Comparison of the S-N curves of the different experiments and numerical results.

model the fatigue behavior of brittle materials based on a variational phase-field approach, *Computer Methods in Applied Mechanics and Engineering* **361**: 112731.

- [3] S. Yan, C. Schreiber, and R. Müller, 2022, An efficient implementation of a phase field model for fatigue crack growth, *International Journal of Fracture* **237**: 47–60.
- [4] Y.-S. Lo, M. J. Borden, K. Ravi-Chandar, and C. M. Landis, 2019, A phase-field model for fatigue crack growth, *Journal of the Mechanics and Physics of Solids* **132**: 103684.
- [5] W. Van Paepegem, 2015, The cycle jump concept for modelling high-cycle fatigue in composite materials, V. Carvelli and S. V. Lomov (eds.), *Fatigue of Textile Composites*, Woodhead Publishing, Sawston, Cambridge, pp. 29–55.
- [6] O. Sally, F. Laurin, C. Julien, R. Desmorat, and F. Bouillon, 2020,

An efficient computational strategy of cycle-jumps dedicated to fatigue of composite structures, *International Journal of Fatigue* **135**: 105500.

- [7] S. Haouala and I. Doghri, 2015, Modeling and algorithms for two-scale time homogenization of viscoelastic-viscoplastic solids under large numbers of cycles, *International Journal of Plasticity* **70**: 98–125.
- [8] S. Yang and Y. Shen, 2023, An acceleration scheme for the phase field fatigue fracture simulation with a concurrent temporal homogenization method, *Computer Methods in Applied Mechanics and Engineering* **416**: 116294.
- [9] R. Behnke, I. Wollny, F. Hartung, and M. Kaliske, 2019, Thermo-mechanical finite element prediction of the structural long-term response of asphalt pavements subjected to periodic traffic load: Tire-

- pavement interaction and rutting, *Computers and Structures* **218**: 9–31.
- [10] R. Behnke and M. Kaliske, 2018, Square block foundation resting on an unbounded soil layer: Long-term prediction of vertical displacement using a time homogenization technique for dynamic loading, *Soil Dynamics and Earthquake Engineering* **115**: 448–471.
- [11] J. Storm, B. Yin, and M. Kaliske, 2022, The concept of Representative Crack Elements (RCE) for phase-field fracture: transient thermo-mechanics, *Computational Mechanics* **69**: 1–12.
- [12] J. Storm, D. Supriatna, and M. Kaliske, 2020, The concept of representative crack elements for phase-field fracture: Anisotropic elasticity and thermo-elasticity, *International Journal for Numerical Methods in Engineering* **121**: 779–805.
- [13] R. Pina-Torres, D. Zhao, J. Storm, and M. Kaliske, 2024, Time homogenization: an acceleration scheme for phase-field modeling of fatigue, submitted for publication.
- [14] S. Goel and S. Singh, 2014, Fatigue performance of plain and steel fibre reinforced self compacting concrete using S–N relationship, *Engineering Structures* **74**: 65–73.
- [15] Y. Xu and Q. Xu, 2023, Experimental study on fatigue damage of self-compacting concrete of CRTS III slab track, *Structures* **53**: 62–69.
- [16] N. Ganesan, J. Bharati Raj, and A. Shashikala, 2013, Flexural fatigue behavior of self compacting rubberized concrete, *Construction and Building Materials* **44**: 7–14.